

# Investigating the Nature of Palladium Chain-Walking in the Enantioselective Redox-Relay Heck Reaction of Alkenyl Alcohols

Margaret J. Hilton,<sup>†</sup> Li-Ping Xu,<sup>‡</sup> Per-Ola Norrby,<sup>§</sup> Yun-Dong Wu,<sup>‡</sup> Olaf Wiest,<sup>‡,||</sup> and Matthew S. Sigman<sup>\*,†</sup>

<sup>†</sup>Department of Chemistry, University of Utah, 315 South 1400 East, Salt Lake City, Utah 84112, United States

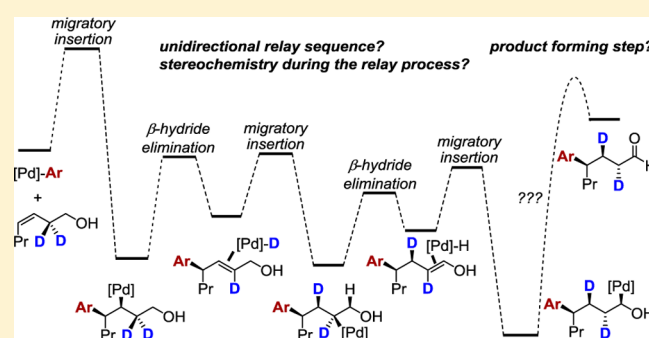
<sup>‡</sup>Laboratory of Computational Chemistry and Drug Design, Laboratory of Chemical Genomics, Peking University Shenzhen Graduate School, Shenzhen 518055, China

<sup>§</sup>Pharmaceutical Development, Global Medicines Development, AstraZeneca, Pepparedsleden 1, SE-431 83 Mölndal, Sweden

<sup>||</sup>Department of Chemistry and Biochemistry, University of Notre Dame, Notre Dame, Indiana 46556, United States

## S Supporting Information

**ABSTRACT:** The mechanism of the redox-relay Heck reaction was investigated using deuterium-labeled substrates. Results support a pathway through a low energy palladium–alkyl intermediate that immediately precedes product formation, ruling out a tautomerization mechanism. DFT calculations of the relevant transition structures at the M06/LAN2DZ+f/6-31+G\* level of theory show that the former pathway is favored by 5.8 kcal/mol. Palladium chain-walking toward the alcohol, following successive  $\beta$ -hydride eliminations and migratory insertions, is also supported in this study. The stereochemistry of deuterium labels is determined, lending support that the catalyst remains bound to the substrate during the relay process and that both *cis*- and *trans*-alkenes form from  $\beta$ -hydride elimination.



## INTRODUCTION

The enantioselective redox-relay Heck reaction yields an aryl–alkyl bond and repositions unsaturation from an alkene to an alcohol (Figure 1).<sup>1–3</sup> These reactions proceed in excellent enantioselectivity with a wide range of aryl-coupling partners as well as differing chain lengths between the alkene and the alcohol in the substrate. The site selectivity in terms of where the aryl group is introduced onto the alkene is sensitive to the nature of both coupling partners.<sup>2,4</sup> The reaction has been optimized using both diazonium salts<sup>1</sup> and boronic acids<sup>2</sup> as the aryl source and is also effective in producing quaternary centers with high enantiomeric ratios starting from trisubstituted alkenol substrates.<sup>5</sup>

Computational studies of the mechanism of the reaction revealed the influences on enantioselectivity and site selectivity.<sup>6,7</sup> A rate-limiting migratory insertion of the arene leads to a relatively shallow region of the potential energy surface for the relay process, which involves the Pd-catalyst migrating or walking toward the alcohol via successive  $\beta$ -hydride eliminations and migratory insertions (Figure 2). Enantioselectivity is attributed in both studies to the steric repulsion of the substrate with the <sup>t</sup>Bu group on the oxazoline portion of the ligand. These interactions lead to high enantiomeric ratios of the products in all cases, indicating that the identity of either coupling partner has little influence over the enantioselectivity-determining step. The catalyst

preferentially binds to one face of the alkene to form the alkyl–aryl bond at the distal  $sp^2$  carbon to the alcohol, leading to the major product (the  $\gamma$ -product for homoallylic alcohols). When the alkene binds to the metal on the opposite face, migratory insertion of the aryl group at the proximal  $sp^2$  carbon results in the enantiomeric  $\beta$ -product. Additionally, (*E*)- and (*Z*)-alkenyl alcohol substrates generate enantiomers.<sup>1,2</sup>

The site selectivity of the reaction is controlled by subtle polarity differences of the alkene carbons in the transition state. The trends in site selectivity are correlative to the polarity differences in alkenes as determined by <sup>13</sup>C NMR shifts,<sup>2</sup> IR C=C stretches,<sup>4</sup> and NBO charges.<sup>7</sup> Furthermore, the site selectivity is also related to the electron density in the aryl coupling partner, as previously demonstrated in a Hammett relationship<sup>2</sup> as well as IR frequencies and intensities.<sup>4</sup> Increased site selectivity is observed with electron-poor aryl groups, bulkier substituents at R', and shorter alkyl chain lengths (Figure 1).

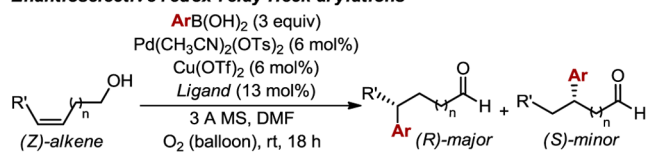
While the two computational studies agree on the major features of the pathway, there are distinct differences proposed for the formation of the carbonyl product from the palladium–enol species (right part of Figure 2). Wang et al. propose the

**Special Issue:** Mechanisms in Metal-Based Organic Chemistry

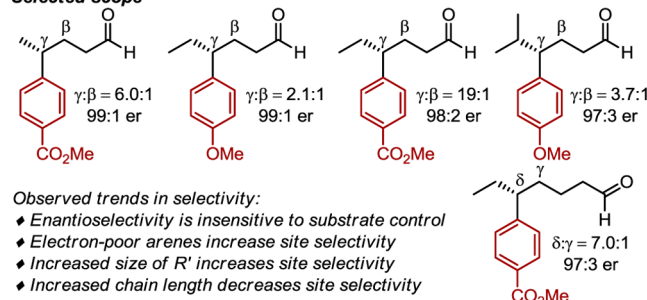
**Received:** August 5, 2014

**Published:** September 4, 2014

## Enantioselective redox-relay Heck arylations



## Selected scope



## Observed trends in selectivity:

- ◆ Enantioselectivity is insensitive to substrate control
- ◆ Electron-poor arenes increase site selectivity
- ◆ Increased size of  $R'$  increases site selectivity
- ◆ Increased chain length decreases site selectivity

## General mechanistic proposal

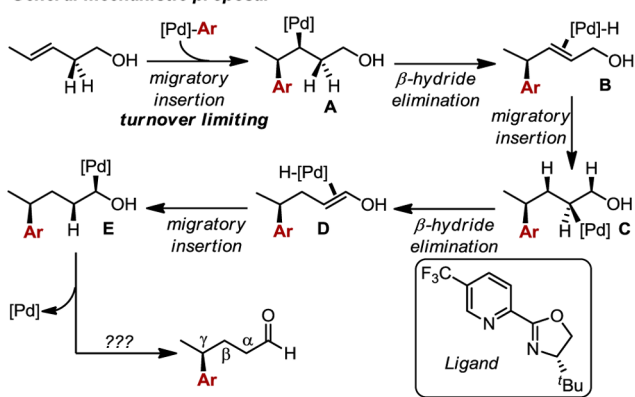


**Figure 1.** Oxidative enantioselective redox-relay Heck reaction details and proposed mechanism.

direct deprotonation of the hydride by DMF,<sup>6</sup> while our studies indicate a reinsertion of the palladium hydride followed by oxidative deprotonation.<sup>7</sup> As the formation of the final product is essential for a complete understanding of the mechanism of the redox-relay Heck reaction, studies to distinguish these two possibilities are desirable.

Herein, we report an investigation regarding the nature of the relay process, including the possibility of reversible chain-

walking and the question of stereochemistry of the palladium-alkyl and -alkenyl intermediates as the catalyst proceeds toward the alcohol. The energy barriers calculated for the relay sequence are relatively modest, suggesting that any  $\beta$ -hydride elimination or migratory insertion step during this process may be readily reversible.<sup>8–10</sup> This poses a number of questions that are important for the selectivity of these steps: (i) which hydrogens are eliminated, (ii) where do the migratory insertions take place, and (iii) does the palladium chain-walking process occur by a reversible, bidirectional mechanism? Poor selectivity during the  $\beta$ -hydride elimination steps could result in mixtures of (*E*)- and (*Z*)-alkenes, although only (*E*)-isomers were considered in the calculations shown in Figure 2. Additionally, reversible binding of these alkenes could cause erosion in the observed enantioselectivity if the face by which the alkene is bound to the metal switches via dissociative/associative processes. Migratory insertion of the palladium hydride could then occur to the opposite prochiral face of the alkene. Thus, the stereochemical integrity of these steps is of significant interest. Finally, we will study the formation of the carbonyl product. In addition to the differences found in the two computational studies, it is noteworthy that substrates with a greater distance (three to five carbons) between the alkene and alcohol form aldehydes and ketones. In case of the minor products resulting from a migratory insertion of the aryl group at the proximal  $\text{sp}^2$  carbon to the alcohol, the catalyst is required to migrate through an already established aryl-alkyl bond to yield the carbonyl product. Irrespective of a reversible relay sequence, it must be favorable for the catalyst to form aldehydes and ketones under standard reaction conditions. It is unclear if the driving force for this depends on the electronic effect of the alcohol or an interaction between the alcohol and the catalyst. In the present study, we will probe the steps of the reaction relevant to these questions through isotopic labeling studies and computational methods.

## RESULTS AND DISCUSSION

## Investigating the Reversibility of the Relay Process.

After the initial migratory insertion of the alkene into the Pd-aryl species to form intermediate A (Figure 2), the barriers between the iterative  $\beta$ -hydride eliminations and migratory insertions are relatively low, suggesting that the catalyst could

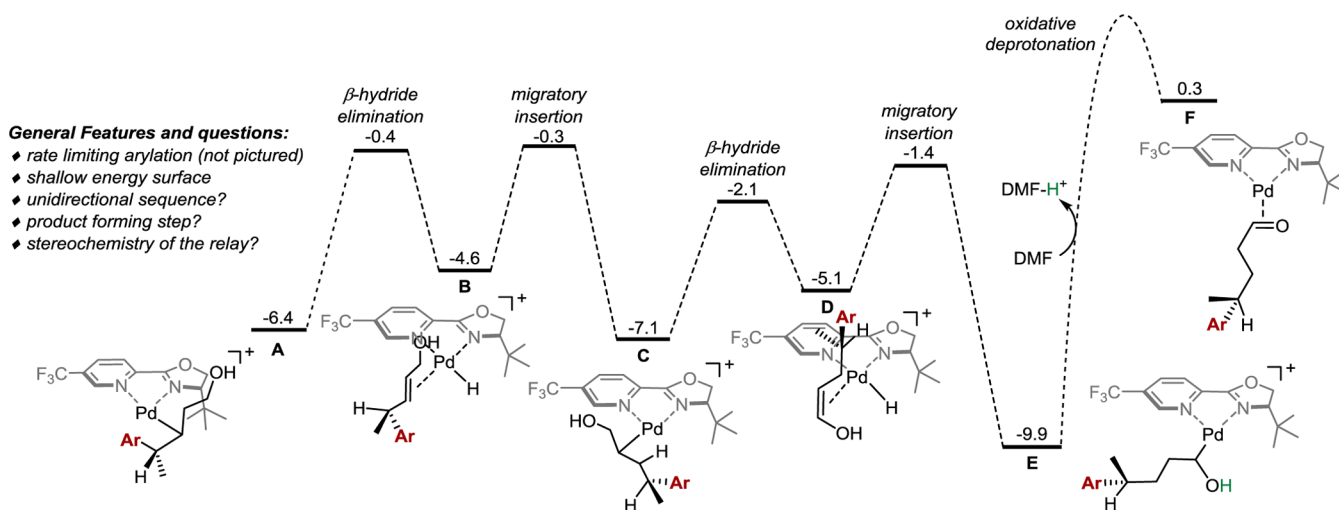
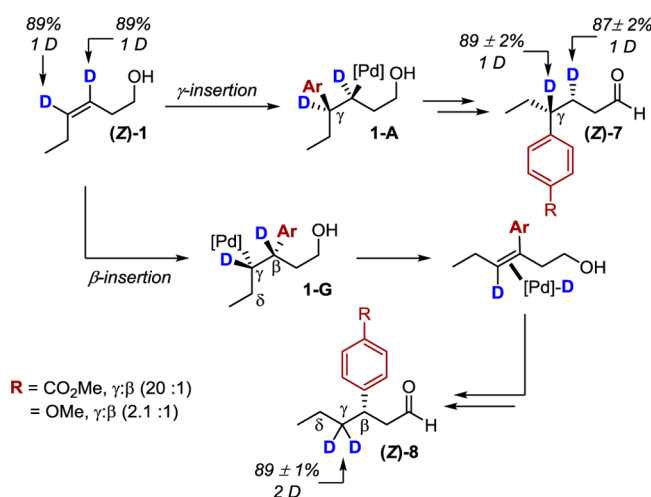


**Figure 2.** Truncated reaction profile from calculated intermediates for major product formation in the redox-relay Heck reaction.

migrate both away from and toward the alcohol before releasing the product. To test this possibility, we synthesized several deuterium-labeled substrates and submitted them to our standard conditions for the oxidative redox-relay Heck reaction (see the conditions in Figure 1). Both (*Z*)- and (*E*)-labeled alkenes were evaluated using electron-rich and electron-poor arenes so that both the  $\beta$ - and  $\gamma$ -products could be readily analyzed (Scheme 1 and Scheme S1, Supporting Information,

**Scheme 1. Evaluation of Deuterium Labels and Site Selectivity Resulting from (*Z*)-Labeled Alkene**



respectively). Electron-poor aryl substrates, such as the *p*-MeO<sub>2</sub>CPhB(OH)<sub>2</sub> used in most studies reported here, yield a higher ratio of the major product with the migratory insertion of the aryl group occurring at the  $\gamma$ -carbon as shown in Figure 2. Conversely, electron-rich arenes, such as the *p*-MeOPhB(OH)<sub>2</sub>, lead to poorer site selectivity, thus allowing analysis of the minor  $\beta$ -product. As shown in Figure 2, insertion of the aryl group at the  $\gamma$ -position leads to the major product in homoallylic alcohol substrates via intermediate A with a palladium–alkyl bond at the  $\beta$ -position. From this intermediate,  $\beta$ -hydride elimination can occur either toward the alcohol to begin the relay process or toward the aryl group. The barrier to eliminate the benzylic hydrogen is higher in energy by 0.9 kcal/mol, and the complex resulting from this step is 4.8 kcal/mol higher in energy than complex B.<sup>7</sup> Yet, these calculations do not conclusively eliminate the possibility of this step occurring.

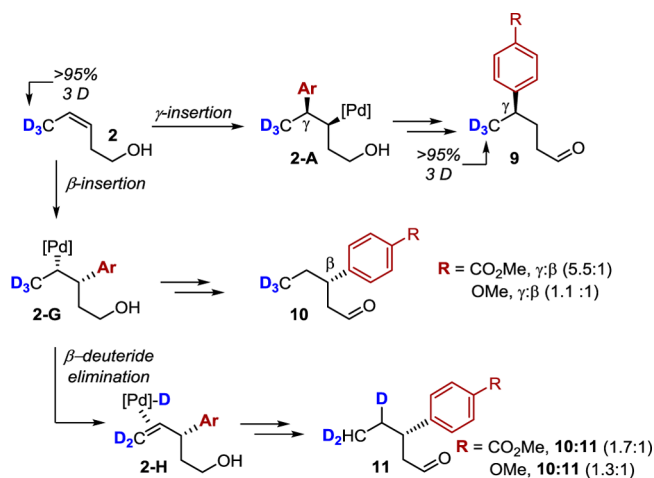
The first substrate examined is (*Z*)-1 (Scheme 1). Preferential insertion at the  $\gamma$ -position relative to the resultant aldehyde product leads to intermediate 1-A, which can undergo  $\beta$ -deuteride elimination at the benzylic  $\gamma$ -position or  $\beta$ -hydride elimination at the  $\alpha$ -position to begin the relay process. If the catalyst migrates away from the alcohol beyond the aryl group, loss of deuterium incorporation at the  $\gamma$ - and  $\beta$ -positions would be expected in the products. Additionally, any incorporation of deuterium at the  $\alpha$ -position would indicate that chain-walking is reversible from 1-A. Experimentally, retention of the deuterium labels at the  $\gamma$ - and  $\beta$ -positions was observed for the major product (*Z*)-7. This suggests that after formation of 1-A, the catalyst preferentially walks toward the alcohol, in agreement with the computationally derived kinetic barrier differences.

An alternative explanation for the preferential formation of (*Z*)-7 is a kinetic isotope effect (KIE) rather than the directionality of the hydrogen elimination. We tested this

possibility by calculating the KIE for the elimination of the  $\beta$ -hydrogen using the free energies for the two isotopomers of the previously described transition structure<sup>7</sup> for this step as described in the Supporting Information. The calculated isotope effect of  $k_{\text{H}}/k_{\text{D}} = 2.66$  is too small to account for the high retention of deuterium incorporation in the formation of (*Z*)-7, confirming the preferential directionality of  $\beta$ -hydride elimination. Insertion of the aryl group at the  $\beta$ -position leads to intermediate 1-G with the palladium–alkyl bond at the  $\gamma$ -position (Scheme 1). Again, the catalyst may eliminate a hydrogen or deuterium either away from or toward the alcohol, respectively. In both cases, the catalyst must migrate through the chiral center to yield the aldehyde product. Thus, the deuterium at the benzylic position will be eliminated and subsequently reinserted at the  $\gamma$ -position. If the catalyst first shifts away from the alcohol in intermediate 1-G, then some migration of deuterium from the  $\gamma$ -position to the  $\delta$ -position would be expected. Product 8 is observed with no detectable hydrogens at the  $\beta$ - or  $\delta$ -position, strongly suggesting that  $\beta$ -hydride elimination occurs toward the benzylic position. This is in line with the previously described polarization in the transition state based on the dipole moment of the C–O directing the relay process toward the alcohol.<sup>7</sup> Nearly identical results were observed for the (*E*)-deuterium labeled alkene (Scheme S1, Supporting Information).

To further probe the directionality of palladium chain-walking, substrate 2 was submitted to the same reaction conditions using an electron-poor and electron-rich coupling partner (Scheme 2). With deuterium labels at the terminal

**Scheme 2. Assessment of Chain-Walking Away from the Alcohol**



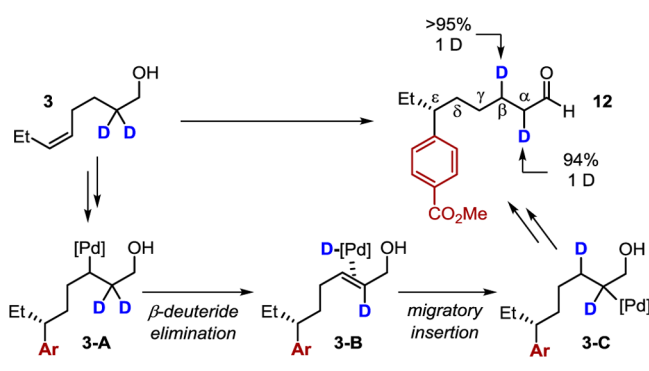
allylic position, any incorporation of hydrogens at this site in either the major or minor product will indicate that an intermediate undergoes  $\beta$ -hydride eliminations away from the alcohol. When the aryl group is inserted at the  $\gamma$ -carbon of 2 to give intermediate 2-A, only  $\beta$ -hydride elimination toward the alcohol results, thus preserving the deuterium labels at the methyl group and yielding product 9.

After the insertion of the aryl group at the  $\beta$ -carbon, producing intermediate 2-G, deuterium scrambling in a  $\sim 1.5:1$  ratio is observed (compare products 10 and 11). Starting from 2-G, elimination of either a hydrogen from the benzylic position or a deuterium from the methyl group can occur. The relay process yields product 10 after elimination of the benzylic

hydrogen. When a  $\beta$ -deuteride elimination at the methyl group occurs to form putative intermediate 2-H, a migratory insertion of the deuterium follows to give a palladium–alkyl species at the terminal carbon. The relay sequence from this complex ultimately leads to product 11. It should be noted that all of the deuterium atoms can be accounted for in the product ruling out any H–D exchange processes. In comparing this to the formation of 8, in which no deuterium incorporation was detected at the  $\delta$ -position, this example shows a significant amount of Pd-walking away from the alcohol. Thus, migration through the benzylic position provides enough hindrance to allow reversible chain-walking away from the alcohol, resulting in deuterium scrambling. Nonetheless, a driving force remains to direct chain-walking toward the alcohol as aldehyde product 11 is still formed.

Lastly, we evaluated the reaction of substrate 3 with deuterium labels remote to both the alkene and the alcohol under the same reaction conditions (Scheme 3). If deuterium is

Scheme 3. Probing the Reversibility of the Relay Process



incorporated elsewhere in the alkyl chain (i.e., in the  $\gamma$ -,  $\delta$ -, or  $\epsilon$ -positions), then the only explanation would be that the catalyst walks reversibly along the chain until product is released. In contrast, if the same bias as discussed above is observed for chain-walking toward the alcohol, then deuterium should only be detected at the  $\alpha$ - and  $\beta$ -positions. Once intermediate 3-A is formed by the initial migratory insertion and relay sequence, a  $\beta$ -deuteride elimination occurs, yielding intermediate 3-B, followed by a migratory insertion of the deuterium to give complex 3-C. The product of this sequence, 12, which retains one deuterium at the  $\alpha$ -position and incorporates one deuterium at the  $\beta$ -position, is the only product observed in the reaction resulting from insertion of the aryl group at the  $\epsilon$ -position. No deuterium incorporation was detected beyond the  $\beta$ -position. Accordingly, the catalyst performs an irreversible sequence of  $\beta$ -deuteride elimination and migratory insertion steps from 3-A to 3-C to eventually yield 12, although the microscopic reversibility of individual steps (i.e., 3-B to 3-A) cannot be ruled out. The lack of detectable deuterium scrambling observed in these studies supports a unidirectional palladium chain-walking leading to the energetically favorable formation of the carbonyl product.

**Examining the Product-Releasing Step(s).** The results discussed above indicate that unidirectional migration ultimately leads to the formation of the carbonyl products. Two different proposals for eventual formation of the carbonyl were reported and are compared in Figure 3. Wang and co-workers suggested<sup>6</sup> that once the palladium–enol intermediate D is reached, a DMF molecule deprotonates the hydride, which

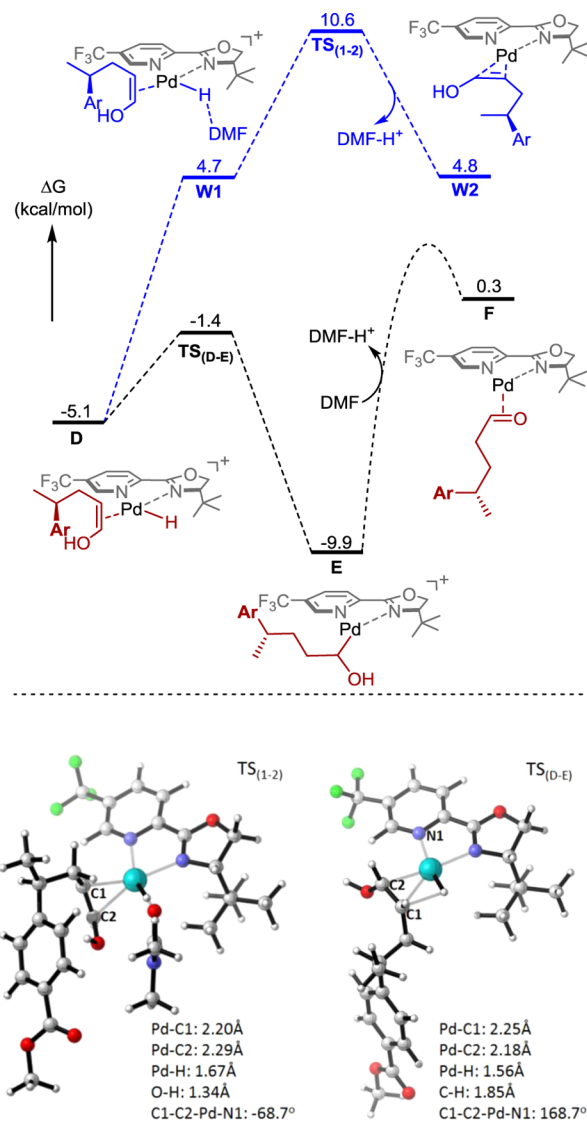


Figure 3. Comparison of the proposed product releasing steps.

allows a palladium-assisted tautomerization to occur via W1 and W2, affording the carbonyl product. Alternatively, we proposed a migratory insertion of the hydride in complex D to yield the palladium–alkyl intermediate E, which then undergoes an oxidative deprotonation by DMF to close the catalytic cycle and release product.<sup>7</sup>

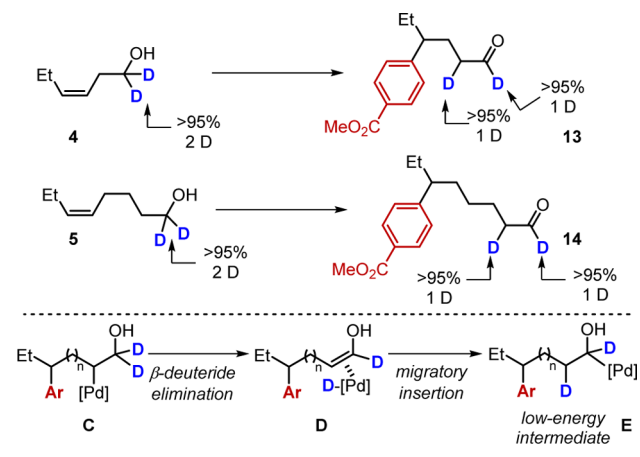
To compare these two possibilities, we calculated both pathways at the M06/LAN2DZ+f/6-31+G\* level of theory used previously.<sup>7</sup> The results, summarized in Figure 3, show that the deprotonation of D by DMF has an activation barrier of 15.7 kcal/mol, which is significantly less favorable than the reinsertion and oxidative deprotonation pathway (12 kcal/mol lower in energy). This is consistent with the hydridic character of the hydrogen in D causing the coordination of DMF to be endergonic by 9.8 kcal/mol. As a result, deprotonation by the weak base DMF ( $pK_a$  of  $DMF-H^+ = -0.01$ )<sup>11</sup> is overall endergonic by 9.9 kcal/mol. In comparison, the activation free energy of the reinsertion is 3.7 kcal/mol, which is consistent with the barriers calculated for the chain walking process, leading to intermediate E. Calculations of the protonation of DMF by E show a monotonous increase in energy. This is indicative of a diffusion-controlled situation where the free

energy barrier to the backward reaction is ca. 4.5 kcal/mol higher than the separated  $F + \text{DMF-H}^+$ , that is, a transition state with a free energy of  $\sim 4.8$  kcal/mol.<sup>12</sup> Identical behavior is seen in model calculations of  $\text{DMF-H}^+$  combined with, for example, a fluoride anion.

The transition structures for the two pathways are shown at the bottom of Figure 3. Consistent with the endergonic nature of the reaction,  $\text{TS}_{(1-2)}$  is a late transition structure with a long Pd–H and a short O–H bond. The dihedral angle C1–C2–Pd–N1 is  $-68.7^\circ$  in  $\text{TS}_{(1-2)}$ , positioning the planes of the ligand and the substrate almost perpendicular to each other to allow the approach of the DMF base. In contrast,  $\text{TS}_{(D-E)}$  is an early transition structure with an extensively elongated C–H bond of 1.85 Å and a nearly square planar environment with a dihedral angle of  $168.7^\circ$ , which contributes to the lower energy of this transition state.

Considering that the energy of the transition structure connecting E and F could not be conclusively established, homoallylic alcohol **4** and tris-homoallylic alcohol **5** were submitted to standard conditions (Scheme 4) to differentiate

Scheme 4. Interrogation of the Product-Forming Step(s)



the two possible pathways experimentally. In both cases, incorporation of one deuterium at the  $\alpha$ -position and retention of one deuterium at the aldehyde are observed. The mechanism that is most consistent with these data is a  $\beta$ -deuteride elimination from the palladium alkyl intermediate **C** yielding the palladium–deuteride complex **D**. Subsequent migratory insertion of the deuteride and oxidative deprotonation from complex **E** would give the observed products **13** and **14**. If a tautomerization mechanism occurred, incorporation of deuterium at the  $\alpha$ -position would not be detected. Thus, the results illustrate that the reaction proceeds through a palladium alkyl intermediate analogous to complex **E** in order to lead to a carbonyl product.

The computational results indicate that **E** is approximately 5 kcal/mol lower in energy than the preceding complex **D**.<sup>7</sup> It is also the lowest energy intermediate calculated along the reaction coordinate. With no detectable deuterium incorporation beyond the  $\alpha$ -carbon in products **13** and **14**, palladium chain-walking is likely irreversible as soon as this species is reached. As previously mentioned, the relay process occurs in one direction, toward the alcohol leading to the formation of this low energy intermediate. Thus, reaching complex **E** can be considered as a thermodynamic driver of this process.

**Stereochemistry of the Relay Process.** As the final set of analyses, we explored the stereochemical integrity of the relay process. Determining whether the catalyst remains on the same side of the alkyl chain throughout the relay process would lend insight into the stereochemistry of the palladium–alkyl intermediates following migratory insertion. By establishing which hydrogens are eliminated during  $\beta$ -hydride elimination(s), the alkene isomers formed during chain-walking can be determined. As reported in previous studies, (*E*)- and (*Z*)-alkenes return enantiomeric products.<sup>1,2</sup> The stereochemistry at both alkene carbons is set by the catalyst during the migratory insertion of the aryl group, as shown in intermediates **1-A** (Figure 4). Thus, we would expect the deuterium labels at the

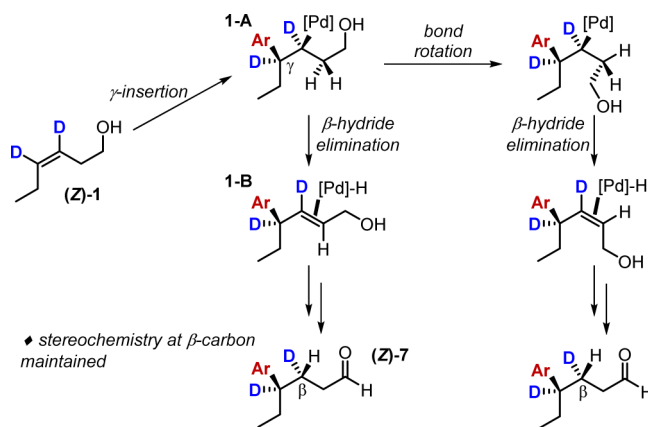


Figure 4. Comparison of the formation of *cis*- and *trans*-alkenes during the relay process.

$\beta$ -centers to exhibit high diastereomeric ratios (dr) if the first migratory insertion was the only observed step in the reaction. However, the stereochemistry of the relay sequence could affect the observed dr. If the catalyst remains bound to the alkene in complex **1-B**, then the hydride will be inserted on the same face of the alkene and the relay process will continue as outlined in Figure 4, yielding product (*Z*)-**7** with the designated stereochemistry, regardless of the types of alkenes formed during the process. In other words, the stereochemistry set by the initial migratory insertion should be retained at the  $\beta$ -position, if a Pd–H species does not dissociate, bind the alkene on the opposite face, and insert the hydrogen from this face. Since we previously did not detect a loss of deuterium incorporation during the formation of Pd–D species, a dissociation/association process by the catalyst is unlikely. Indeed, when comparing the  $^1\text{H}$  NMR spectra of the products resulting from the reaction of substrates (*Z*)-**1** and (*E*)-**1**, it was noted that distinct peaks are present for the protons at the  $\beta$ -position, which supports the retention of alkene face selection by the catalyst in intermediates **1-B**. In order to confirm this hypothesis, we set out to determine the relative stereochemistry of the protons at the  $\beta$ -position.

The product of the redox relay Heck reaction was converted to the tetralone derivative **15** through oxidation and Friedel–Crafts acylation (Figure 5). The relative stereochemistry of each distinct hydrogen in the six-membered ring of **15** can be related to their respective peaks in the  $^1\text{H}$  NMR spectrum. To confirm our assignment, a designated protocol, which included a conformational analysis, geometry optimization of each conformer, NMR shielding tensors calculations, and Boltzmann weighting of these tensors, was followed to determine NMR

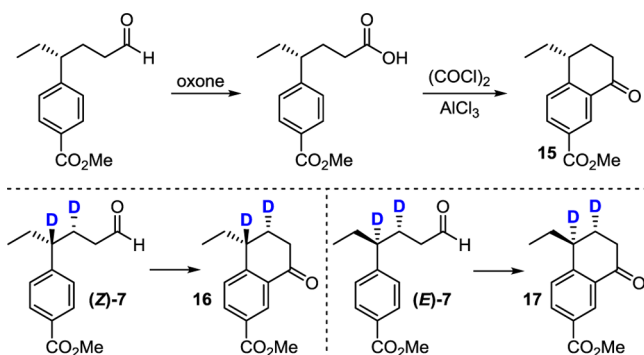


Figure 5. Determination of stereochemistry of deuterium labels.

shifts computationally (see the Supporting Information).<sup>13</sup> Calculated NMR shifts and coupling constants agreed well with experimental values. Products (*Z*)-7 and (*E*)-7 were also transformed into tetralone derivatives **16** and **17** to allow the analysis of their <sup>1</sup>H NMR spectra and thus the determination of the stereochemistry of the deuterium labels. The characterization of **16** and **17** demonstrates unequivocally that the stereochemistry is conserved during the chain walking process as outlined in Figures 4 and 5. This agrees with a deuterium labeling study performed in a previous report,<sup>5</sup> where the stereochemical integrity of a substrate containing a preinstalled chiral center was maintained during the relay process. Additionally, this explains why the observed enantioselectivity of the minor  $\beta$ -products are high and do not erode during the relay sequence.

These findings confirm our hypothesis that the catalyst does not dissociate and associate from the substrate during the relay sequence. Interestingly, as palladium remains bound to one face of the alkene, the stereochemistry of the  $\beta$ -center is not affected by the type of alkenes formed after the first  $\beta$ -hydride elimination in intermediates **1-B** (Figure 4), yet the alkene isomers formed during the relay process should affect the diastereomeric ratio of the  $\alpha$ -position.

To interrogate the stereochemistry of the alkene isomer(s) formed from the initial  $\beta$ -hydride elimination, substrate **6** was subjected to the same reaction conditions and ultimately converted into **20** and **21** (Figure 6). While the stereocenter at the  $\beta$ -position is formed in high fidelity as predicted, the stereocenter at the  $\alpha$ -position is formed as a 1.3:1 mixture of

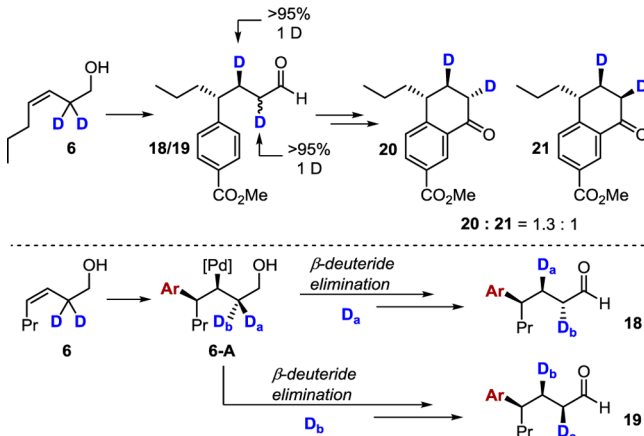


Figure 6. Stereochemical outcome resulting from the relay process and mechanistic analysis.

diastereomers. If the catalyst eliminates  $D_a$  from intermediate **6-A**, this leads to a *trans*-alkene and *anti*-orientation of the deuterium labels (Figure 6). To eliminate  $D_b$ , a bond rotation must first take place, as previously discussed (Figure 4). A *cis*-alkene forms, and palladium chain-walking yields a *syn*-orientation of the deuterium labels. The steric repulsion between the alcohol and the opposite end of the alkyl chain is not sufficient to limit the bond rotation, as the observed diastereomeric ratio is low. Consequently, *cis*- and *trans*-alkenes form in nearly equal amounts from the initial  $\beta$ -hydride elimination during the relay process in homoallylic alcohols. It is possible that with a bulkier alkyl chain, the barrier to bond rotation would become too large, limiting the formation of the *cis*-alkene. Nevertheless, the catalyst remains on the same side of the substrate throughout the relay process, as demonstrated by the uniform stereochemistry at the  $\beta$ -position in products **20** and **21**.

In summary, we have provided experimental and computational evidence elucidating the chain-walking and product-forming steps of the redox-relay Heck reaction. The transformation proceeds through iterative  $\beta$ -hydride elimination and migratory insertion steps until arriving at a low energy palladium–alkyl intermediate, as demonstrated by the series of deuterium-labeling studies presented. Reaching this low energy complex is proposed to be a driving force for directing the catalyst toward the alcohol and toward the formation of carbonyl products. During the relay sequence, the face selection of the alkene by the catalyst remains consistent, indicating that it remains bound to the substrate. Additionally, both (*E*)- and (*Z*)-alkene isomers form during the relay process. Finally, the product-forming step was shown to proceed from the migratory insertion cascade by deprotonation of the low energy intermediate rather than a deprotonation of the palladium hydride species by DMF. Future studies look to take advantage of these insights in the continued development of relay Heck processes.

## EXPERIMENTAL SECTION

**General Methods.** Dry dimethylformamide (DMF) was stored over activated 3 Å molecular sieves (3 Å MS). Powdered 3 Å MS were activated by flowing  $N_2$  through a glass tube filled with sieves maintained at 200 °C.  $Pd(CH_3CN)_2(OTf)_2$  and the pyrox ligand were synthesized according to literature procedures.<sup>1,14</sup> Spectra of the deuterium-labeled substrates were compared to previously characterized or commercially available substrates without deuterium labels. Spectra of the resulting products were compared to previously characterized products.<sup>1,2</sup> <sup>1</sup>H NMR spectra were obtained at 300, 500, or 800 MHz; chemical shifts are reported in ppm and referenced to the  $CHCl_3$  singlet at 7.26 ppm. <sup>13</sup>C NMR spectra were obtained at 125 MHz and referenced to the center peak of the  $CDCl_3$  triplet at 77.00 ppm. The abbreviations s, d, t, q, quin, sext, dd, dt, and m stand for the resonance multiplicities singlet, doublet, triplet, quartet, quintet, sextet, doublet of doublets, doublet of triplets, and multiplet, respectively.

**Synthesis of Deuterium-Labeled Substrates.** (*Z*)-Hex-3-en-3,4- $d_2$ -1-ol ((*Z*)-1). To reduce 3-hexyn-1-ol (0.42 g, 4.3 mmol), a previously reported procedure was employed using  $Ni(OAc)_2$ ,  $NaBD_4$ ,  $D_2$  (balloon),  $D_2O$ , and  $MeOD-d_4$ .<sup>1</sup> A clear oil was isolated after flash chromatography in 48% yield (0.22 g): <sup>1</sup>H NMR ( $CDCl_3$ , 500 MHz)  $\delta$  = 3.63 (t,  $J$  = 6.5 Hz, 2 H), 2.32 (t,  $J$  = 6.5 Hz, 2 H), 2.03 (q,  $J$  = 7.5 Hz, 2 H), 1.51 (bs, 1 H), 0.97 (t,  $J$  = 7.5, 3 H) ppm.

(*E*)-Hex-3-en-3,4- $d_2$ -1-ol ((*E*)-1). To a dry 100 mL round-bottom flask was added lithium aluminum deuteride (LAD) (0.54 g, 13.2 mmol, 2 equiv). The flask was fitted with a reflux condenser, and the apparatus was purged with nitrogen. Dry THF (40 mL) was added, and the flask was cooled in an ice bath. To this was added 3-hexyn-1-ol (0.65 g, 6.6 mmol) dissolved in THF (10 mL). The reaction mixture

was allowed to reflux until full consumption of the alkyne, determined by  $^1\text{H}$  NMR. The reaction was cooled in an ice bath and was quenched with  $\text{D}_2\text{O}$  (15 mL). The layers were separated, and the aqueous layer was extracted with diethyl ether ( $2 \times 15$  mL). The combined organic layers were washed with brine ( $3 \times 15$  mL), dried over magnesium sulfate, and concentrated under reduced pressure. The deuterated *trans*-alkene was isolated as a clear oil in 74% yield (0.50 g):  $^1\text{H}$  NMR ( $\text{CDCl}_3$ , 500 MHz)  $\delta = 3.62$  (t,  $J = 7.5$ , 2 H), 2.26 (t,  $J = 6.5$  Hz, 2 H), 2.03 (q,  $J = 7.5$  Hz, 2 H), 1.41 (bs, 1 H), 0.98 (t,  $J = 7.5$ , 3 H) ppm.

***tert*-Butyldimethyl(pent-3-yn-5- $d_3$ -1-yloxy)silane.** To a dry 250 mL round-bottom flask were added (but-3-yn-1-yloxy)(*tert*-butyl)dimethylsilane (6.36 g, 35.0 mmol) and THF (100 mL). The solution was cooled in a dry ice bath to  $-78$  °C. To this was added *n*-BuLi (16.6 mL, 38.0 mmol, 1.2 equiv), and the reaction was allowed to stir for 2 h. Iodomethane- $d_3$  (5.00 g, 34.5 mmol) in THF (10 mL) was added to the mixture, which was stirred overnight with warming to room temperature. The reaction was quenched with water (10 mL). The layers were separated, and the aqueous layer was extracted with diethyl ether ( $3 \times 10$  mL). The combined organic layers were washed with brine ( $3 \times 10$  mL), dried over magnesium sulfate, and concentrated under reduced pressure. The product was purified using flash chromatography and recovered in a 79% yield (5.54 g) as a clear oil:  $^1\text{H}$  NMR ( $\text{CDCl}_3$ , 300 MHz)  $\delta = 3.70$  (t,  $J = 7.5$  Hz, 2H), 2.35 (t,  $J = 7.5$  Hz, 2H), 0.91 (s, 9 H), 0.08 (s, 6 H) ppm.

**(*Z*)-Pent-3-en-5- $d_3$ -1-ol (2).** The protected alcohol, *tert*-butyldimethyl(pent-3-yn-5- $d_3$ -1-yloxy)silane (5.54 g, 27.4 mmol), was deprotected using 1 M tetra-*n*-butylammonium fluoride (TBAF) (14.3 mL, 54.8 mmol, 2 equiv) in THF (50 mL). The reaction was allowed to stir overnight and was quenched with water (15 mL). The layers were separated, and the aqueous layer was extracted with diethyl ether ( $3 \times 10$  mL). The combined organic layers were washed with brine ( $3 \times 10$  mL), dried over magnesium sulfate, and concentrated under reduced pressure. The alcohol was carried on without purification. To reduce the alkyne (2.0 g, 23 mmol) to the alkene, a previously reported procedure was used, employing  $\text{Ni}(\text{OAc})_2 \cdot 4\text{H}_2\text{O}$  (1.4 g, 5.7 mmol, 25 mol %),  $\text{NaBH}_4$  (0.22 g, 5.7 mmol, 25 mol %), and  $\text{H}_2$  (balloon).<sup>1</sup> A clear oil was isolated after purification using flash chromatography, eluting with a gradient of 10–30% ethyl acetate in hexanes: yield over two steps 21% (0.52 g);  $^1\text{H}$  NMR ( $\text{CDCl}_3$ , 300 MHz)  $\delta = 5.65$  (d,  $J = 6.3$  Hz, 1 H), 5.42–5.37 (m, 1 H), 3.67 (t,  $J = 6.0$  Hz, 2H), 2.33 (q,  $J = 6.5$  Hz, 2H) ppm.

**Methyl (*Z*)-Oct-5-enoate.** (*Z*)-5-Octenoic acid was prepared according to a previously reported procedure from (*Z*)-oct-5-en-1-ol (5.0 g, 39 mmol), and its purity was confirmed by  $^1\text{H}$  NMR.<sup>15,16</sup> In an ice bath, nitrosomethylurea (3.2 g, 30 mmol, 3 equiv) was dissolved in ether (10 mL) and aqueous 20 wt % KOH (10 mL). The organic phase turned bright yellow upon formation of diazomethane. To a different flask were added (*Z*)-5-octenoic acid (1.9 g, 13 mmol) and ether (10 mL). The organic phase containing diazomethane was transferred dropwise by pipet to the carboxylic acid solution, and the evolution of nitrogen gas was observed. The diazomethane solution was added until the solution remained bright yellow. Excess diazomethane in both solutions was quenched slowly with glacial acetic acid (<1 mL each). The reaction mixture was dried over magnesium sulfate, concentrated under reduced pressure, and purified using flash chromatography. A clear oil was isolated in 38% yield over two steps (2.0 g):  $R_f = 0.69$  (80:20 hexanes/ethyl acetate);  $^1\text{H}$  NMR ( $\text{CDCl}_3$ , 300 MHz)  $\delta = 5.45$ –5.24 (m, 2H), 3.66 (s, 3H), 2.31 (t,  $J = 7.5$  Hz, 2H), 2.08–1.98 (m, 4H), 1.71–1.65 (m, 2H), 0.94 (t,  $J = 7.7$  Hz, 3H) ppm;  $^{13}\text{C}\{^1\text{H}\}$  NMR ( $\text{CDCl}_3$ , 125 MHz)  $\delta = 174.3$ , 132.9, 128.0, 51.6, 33.6, 26.6, 25.1, 20.7, 14.5 ppm; IR (neat) 3005, 2961, 2874, 1737, 1436, 1365, 1206, 1161, 1115, 1050, 953, 885, 864, 797, 702  $\text{cm}^{-1}$ ; HRMS (ESI-TOF)  $m/z$  [ $\text{M} + \text{Na}$ ]<sup>+</sup> calcd for  $\text{C}_9\text{H}_{17}\text{O}_2\text{Na}$  157.1229, found 157.1232.

**(*Z*)-Oct-5-en-2,2- $d_2$ -1-ol (3).** To an oven-dried 50 mL round-bottom flask equipped with a stir bar was added methyl (*Z*)-oct-5-enoate (0.50 g, 3.2 mmol). To this was added a 1 M solution of NaOMe in  $\text{MeOH-}d_4$  (6.4 mL, 6.4 mmol, 2 equiv), which was prepared from sodium and  $\text{MeOH-}d_4$ . The reaction was allowed to stir at room temperature under nitrogen for 18 h. The reaction mixture

was quenched with  $\text{D}_2\text{O}$  (1 mL). Then aqueous ammonium chloride (15 mL) and diethyl ether (15 mL) were added. The layers were separated, and the aqueous layer was extracted with ether ( $2 \times 15$  mL). The combined organic layers were washed with aqueous ammonium chloride ( $3 \times 10$  mL), dried over magnesium sulfate, and concentrated under reduced pressure. To reduce the deuterated ester (0.21 g, 1.4 mmol) to the alcohol,  $\text{LiAlH}_4$  (0.10 g, 2.7 mmol, 2 equiv) was added to a dry 50 mL round-bottom flask, which was subsequently purged with nitrogen. To this, placed in an ice bath, was added THF (10 mL). The deuterated ester was dissolved in THF (5 mL) and added to the flask. The reaction mixture was allowed to stir overnight with warming to room temperature. The reaction was cooled in an ice bath and quenched slowly with water (2 mL) and then 20 wt % aqueous KOH (20 mL). This was allowed to stir for 1 h. The layers were separated in a separatory funnel, and the aqueous layer was extracted with ether ( $3 \times 10$  mL). The combined organic layers were washed with brine ( $3 \times 10$  mL), dried over magnesium sulfate, and concentrated under reduced pressure. A colorless oil was isolated after purification using flash chromatography, eluting with a 10% ethyl acetate in hexanes: yield over two steps 24% (0.10 g);  $^1\text{H}$  NMR ( $\text{CDCl}_3$ , 500 MHz)  $\delta = 5.40$ –5.29 (m, 2H), 3.64 (s, 2H), 2.08–2.00 (m, 4H), 1.40 (t,  $J = 7.5$  Hz, 2H), 0.95 (t,  $J = 7.5$  Hz, 3H) ppm.

**Methyl (*Z*)-Hex-3-enoate.** The carboxylic acid, (*Z*)-3-hexenoic acid, was prepared according to a previously reported procedure from (*Z*)-hex-3-en-1-ol (3.0 g, 30 mmol), and its purity was confirmed by  $^1\text{H}$  NMR.<sup>16</sup> The ester was prepared in the same manner as described for methyl (*Z*)-oct-5-enoate and was purified using flash chromatography eluting with a gradient of 5–20% ethyl acetate to hexanes to give a clear oil in a 37% yield over two steps (1.1 g):  $R_f = 0.72$  (80:20 hexanes/ethyl acetate);  $^1\text{H}$  NMR ( $\text{CDCl}_3$ , 300 MHz) 5.62–5.46 (m, 2H), 3.68 (s, 3H), 3.09 (d,  $J = 6.3$  Hz, 2H), 2.05 (p,  $J = 7.5$  Hz, 2H), 0.97 (t,  $J = 7.5$  Hz, 3H) ppm;  $^{13}\text{C}\{^1\text{H}\}$  NMR ( $\text{CDCl}_3$ , 125 MHz)  $\delta = 172.6$ , 135.3, 120.3, 52.0, 32.9, 20.9, 14.1 ppm; IR (neat) 3025, 2964, 2876, 1738, 1436, 1402, 1330, 1305, 1255, 1162, 1114, 1070, 1018, 982, 933, 893, 870, 844, 692  $\text{cm}^{-1}$ ; HRMS (ESI-TOF)  $m/z$  [ $\text{M} + \text{Na}$ ]<sup>+</sup> calcd for  $\text{C}_9\text{H}_{15}\text{O}_2\text{Na}$  129.0916, found 129.0925.

**(*Z*)-Hex-3-en-1,1- $d_2$ -1-ol (4).** To an oven-dried 50 mL round-bottom flask was added LAD (0.27 g, 6.4 mmol, 2 equiv), which was subsequently purged with nitrogen. The flask was placed in an ice bath, and THF (10 mL) was added. Methyl (*Z*)-hex-3-enoate (0.50 g, 3.2 mmol) was dissolved in THF (10 mL) and added to the reaction flask. The mixture was stirred for 18 h. The reaction was cooled in an ice bath and quenched slowly with water (2 mL) and then 20 wt % aqueous KOH (20 mL). This was allowed to stir for 1 h. The layers were separated in a separatory funnel, and the aqueous layer was extracted with ether ( $3 \times 10$  mL). The combined organic layers were washed with brine ( $3 \times 10$  mL), dried over magnesium sulfate, and concentrated under reduced pressure. The crude mixture was purified using flash chromatography eluting with a gradient of 5–20% ethyl acetate in hexanes to give a clear oil in a 39% yield (0.16 g):  $^1\text{H}$  NMR ( $\text{CDCl}_3$ , 300 MHz)  $\delta = 5.58$ –5.52 (m, 1H), 5.35–5.30 (m, 1H), 2.31 (d,  $J = 7.5$  Hz, 2H), 2.08 (quin,  $J = 7.5$  Hz, 2H), 1.52 (s, 1H), 0.97 (t,  $J = 7.5$  Hz, 3H) ppm.

**(*Z*)-Oct-5-en-1,1- $d_2$ -1-ol (5).** The alcohol was prepared in the same manner as described for (*Z*)-hex-3-en-1,1- $d_2$ -1-ol from the corresponding ester, methyl (*Z*)-oct-5-enoate (0.5 g, 3.2 mmol). A clear oil was isolated in 62% yield (0.26 g) after purification using flash chromatography:  $^1\text{H}$  NMR ( $\text{CDCl}_3$ , 500 MHz)  $\delta = 5.40$ –5.29 (m, 2H), 2.08–2.00 (m, 4H), 1.58–1.55 (m, 2H), 1.44–1.38 (m, 2H), 1.33 (br s, 1H), 0.95 (t,  $J = 7.7$  Hz, 3H) ppm.

**(2-Iodoethoxy-2,2- $d_2$ )methanetriyltribenzene.** Methyl glycolate (1.4 mL, 18 mmol) was protected with trityl chloride (5.2 g, 18 mmol) using a previously reported procedure to yield the protected alcohol.<sup>17</sup> The ester (4.0 g, 12 mmol) was reduced with LAD (0.75 g, 18 mmol) in a procedure as described above for the reduction of methyl (*Z*)-hex-3-enoate and methyl (*Z*)-oct-5-enoate. The free alcohol (3.4 g, 11 mmol) was converted to the corresponding alkyl iodide, according to a previously reported procedure.<sup>18</sup> A white solid was recovered: yield over three steps 53% (4.0 g); mp 128–131 °C;  $R_f = 0.78$  (90:10 hexanes/ethyl acetate);  $^1\text{H}$  NMR ( $\text{CDCl}_3$ , 500 MHz)  $\delta = 7.62$  (d,  $J =$

13.0 Hz, 6 H), 7.45–7.32 (m, 9 H), 3.52 (s, 2H) ppm;  $^{13}\text{C}\{^1\text{H}\}$  NMR ( $\text{CDCl}_3$ , 125 MHz)  $\delta$  = 144.2, 129.0, 128.2, 127.5, 87.3, 64.5 ppm; IR (neat) 2973, 2859, 1490, 1448, 1065, 1032, 1002, 983, 902, 759, 747, 699, 668, 646, 633, 605  $\text{cm}^{-1}$ ; HRMS (ESI-TOF)  $m/z$  [ $\text{M} + \text{Na}$ ] $^+$  calcd for  $\text{C}_{21}\text{H}_{17}\text{D}_2\text{ONa}$  439.0519, found 439.0519.

**Hept-3-yn-2,2- $d_2$ -1-ol.** Pent-1-yne (1.7 mL, 17 mmol, 3.0 equiv) was dissolved in THF (50 mL) and cooled to 0 °C. To this was added *n*-BuLi (8.5 mmol, 3.5 equiv), and the mixture was allowed to stir for 2 h. To this was added ((2-iodoethoxy-2,2- $d_2$ )methanetriyl)tribenzene (2.3 g, 5.6 mmol) dissolved in THF (10 mL) and hexamethylphosphoramide (2.9 mL, 17 mmol, 3.0 equiv). The reaction mixture was allowed to stir overnight and was quenched with water (10 mL). The layers were separated, and the aqueous layer was extracted with diethyl ether (3  $\times$  10 mL). The combined organic layers were washed with brine (3  $\times$  15 mL), dried over magnesium sulfate, and concentrated under reduced pressure. The resulting solid was dissolved in 2:1 DCM/MeOH (20 mL). To this was added *p*-toluenesulfonic acid (1 equiv), and the reaction was allowed to stir overnight. The mixture was quenched with water (10 mL), the layers were separated, and the aqueous layer was extracted with dichloromethane (3  $\times$  10 mL). The combined organic layers were washed with brine (3  $\times$  15 mL), dried over magnesium sulfate, and concentrated under reduced pressure. The free alcohol was purified using flash chromatography to give a colorless oil: yield over two steps 31% (0.20 g);  $^1\text{H}$  NMR ( $\text{CDCl}_3$ , 500 MHz) 3.67 (s, 2H), 2.14 (t,  $J$  = 7.0 Hz, 2 H), 1.76 (bs, 1 H), 1.51 (sext,  $J$  = 7.5 Hz, 2 H), 0.97 (t,  $J$  = 7.0 Hz, 3 H) ppm.

**(*Z*)-Hept-3-en-2,2- $d_2$ -1-ol (6).** Hept-3-yn-2,2- $d_2$ -1-ol (0.20 g, 1.7 mmol) was reduced according to a previously reported procedure using  $\text{Ni}(\text{OAc})_2 \cdot 4\text{H}_2\text{O}$ ,  $\text{NaBH}_4$ , and  $\text{H}_2$  to yield a clear oil:  $^1$  yield 70% (0.14 g);  $^1\text{H}$  NMR ( $\text{CDCl}_3$ , 500 MHz) 5.59–5.54 (m, 1H), 5.37 (d,  $J$  = 10.5 Hz, 1 H), 3.63 (s, 2 H), 2.05 (q,  $J$  = 7.5 Hz, 2 H), 1.38 (sext,  $J$  = 7.5 Hz, 2 H), 0.91 (t,  $J$  = 7.5 Hz, 3 H) ppm.

**General Procedure for Oxidative Heck Reactions.** To a dry 10 mL round-bottom flask equipped with a stir bar was added  $\text{Pd}(\text{CH}_3\text{CN})_2(\text{OTf})_2$  (15.9 mg, 0.0300 mmol, 6.00 mol %),  $\text{Cu}(\text{OTf})_2$  (10.9 mg, 0.0300 mmol, 6.00 mol %), *ligand* (17.7 mg, 0.0650 mmol), and DMF (3 mL). The resulting mixture was stirred for 10 min. To this was added a DMF solution (2 mL) of the alkenyl alcohol (0.500 mmol). To a dry 10 mL round-bottom flask equipped with a stir bar was added the corresponding boronic acid (1.50 mmol, 3 equiv) and 3 Å MS (75.0 mg, 150 mg/mmol), which was subsequently purged with oxygen. The palladium and substrate mixture was added to the flask containing the boronic acid and was stirred at room temperature for 18 h. The mixture was diluted with diethyl ether (20 mL) and water (10 mL). The aqueous layer was extracted with diethyl ether (2  $\times$  15 mL). The combined organic layers were washed with brine (3  $\times$  15 mL), dried over magnesium sulfate, and concentrated under reduced pressure. The crude mixture was purified using flash chromatography. The isolated aldehydes were reduced to alcohols with  $\text{NaBH}_4$  (2 equiv) in MeOH for greater stability. Spectra of the aldehydes and alcohols were compared to previously characterized products without deuterium labels.<sup>2</sup> Labeling experiments were repeated at least two times. Isolated yields are reported with the major product as a mixture of regioisomers.

**(*Z*)-7- $\text{CO}_2\text{Me}$ .** A colorless oil was recovered after flash chromatography: yield 68% (79 mg);  $^1\text{H}$  NMR (300 MHz,  $\text{CDCl}_3$ )  $\delta$  = 9.66 (t,  $J$  = 1.5 Hz, 1 H), 7.97 (d,  $J$  = 8.1 Hz, 2 H), 7.19 (d,  $J$  = 8.1 Hz, 2 H), 3.90 (s, 3 H), 2.34–2.14 (m, 2 H), 2.03 (t,  $J$  = 7.8 Hz, 1 H), 1.78–1.54 (m, 2 H), 0.77 (t,  $J$  = 7.5 Hz, 3 H) ppm; MS (low res) 236.1.

**(*E*)-7- $\text{CO}_2\text{Me}$ .** A colorless oil was recovered after flash chromatography: yield 42% (49 mg);  $^1\text{H}$  NMR (500 MHz,  $\text{CDCl}_3$ )  $\delta$  = 9.66 (t,  $J$  = 1.5 Hz, 1 H), 7.97 (d,  $J$  = 8.5 Hz, 2 H), 7.19 (d,  $J$  = 8.5 Hz, 2 H), 3.90 (s, 3 H), 2.31–2.20 (m, 2 H), 1.80 (t,  $J$  = 7.0 Hz, 1 H), 1.75–1.56 (m, 2 H), 0.77 (t,  $J$  = 7.5 Hz, 3 H) ppm; MS (low res) 236.2.

**(*E*)-8- $\text{CO}_2\text{Me}$ .** A colorless oil was recovered after flash chromatography:  $^1\text{H}$  NMR (500 MHz,  $\text{CDCl}_3$ )  $\delta$  = 9.66 (t,  $J$  = 1.5 Hz, 1 H), 7.97 (d,  $J$  = 8.5 Hz, 2 H), 7.26 (d,  $J$  = 8.0 Hz, 2 H), 3.90 (s, 3 H), 3.24 (t,  $J$  = 7.0, 1 H), 2.73 (dd,  $J$  = 2.0, 7.2 Hz, 2 H), 1.18–1.05 (m, 2H), 0.82 (t,  $J$  = 7.5 Hz, 3 H) ppm; MS (low res) 236.2.

**(*Z*)-7- $\text{OMe}$ .** A colorless oil was recovered after flash chromatography: yield 72% (84 mg).  $^1\text{H}$  NMR (500 MHz,  $\text{CDCl}_3$ )  $\delta$  = 9.64 (t,  $J$  = 1.5 Hz, 1 H), 7.03 (d,  $J$  = 8.5 Hz, 2H), 6.87 (d,  $J$  = 8.5 Hz, 2 H), 3.79 (s, 3 H), 2.31–2.21 (m, 2 H), 1.98 (t,  $J$  = 8.0 Hz, 1 H), 1.70–1.51 (m, 2 H), 0.77 (t,  $J$  = 7.5 Hz, 3 H) ppm; MS (low res) 208.2.

**(*Z*)-8- $\text{OMe}$ .** A colorless oil was recovered after flash chromatography:  $^1\text{H}$  NMR (500 MHz,  $\text{CDCl}_3$ )  $\delta$  = 9.65 (t,  $J$  = 1.5 Hz, 1 H), 7.10 (d,  $J$  = 8.5 Hz, 2H), 6.87 (d,  $J$  = 8.5 Hz, 2 H), 3.78 (s, 3 H), 3.13 (q,  $J$  = 7.0 Hz, 1H), 2.67 (dd,  $J$  = 2.0, 7.0 Hz, 2H), 1.22–1.12 (m, 2 H), 0.85 (t,  $J$  = 7.5 Hz, 3 H) ppm; MS (low res) 208.2.

**(*E*)-7- $\text{OMe}$ .** A colorless oil was recovered after flash chromatography: yield 87% (102 mg);  $^1\text{H}$  NMR (500 MHz,  $\text{CDCl}_3$ )  $\delta$  = 9.64 (t,  $J$  = 1.5 Hz, 1 H), 7.03 (d,  $J$  = 8.5 Hz, 2 H), 6.84 (d,  $J$  = 8.5 Hz, 2 H), 3.77 (s, 3 H), 2.30–2.20 (m, 2 H), 1.73 (t,  $J$  = 7.0 Hz, 1 H), 1.69–1.51 (m, 2 H), 0.77 (t,  $J$  = 7.5 Hz, 3 H) ppm; MS (low res) 208.2.

**(*E*)-8- $\text{OMe}$ .** A colorless oil was recovered after flash chromatography:  $^1\text{H}$  NMR (500 MHz,  $\text{CDCl}_3$ )  $\delta$  = 9.64 (t,  $J$  = 1.5 Hz, 1 H), 7.09 (d,  $J$  = 8.5 Hz, 2 H), 6.84 (d,  $J$  = 8.5 Hz, 2 H), 3.78 (s, 3 H), 3.12 (t,  $J$  = 7.5 Hz, 1H), 2.66 (dd,  $J$  = 2.0, 7.2 Hz, 2H), 1.21–1.13 (m, 2 H), 0.85 (t,  $J$  = 7.0 Hz, 3 H) ppm; MS (low res) 208.2.

**9- $\text{CO}_2\text{Me}$ .** A colorless oil was recovered after flash chromatography: yield 62% (64 mg);  $^1\text{H}$  NMR (500 MHz,  $\text{CDCl}_3$ )  $\delta$  = 9.68 (t,  $J$  = 1.5 Hz, 1 H), 7.97 (d,  $J$  = 8.5 Hz, 2 H), 7.24 (d,  $J$  = 8.0 Hz, 2 H), 3.90 (s, 3 H), 2.80–2.74 (m, 1 H), 2.38–2.18 (m, 2 H), 1.99–1.84 (m, 2H) ppm; MS (low res) 223.1.

**9- $\text{OMe}$ .** A colorless oil was recovered after flash chromatography: yield 72% (75 mg);  $^1\text{H}$  NMR (500 MHz,  $\text{CDCl}_3$ )  $\delta$  = 9.65 (t,  $J$  = 2.0 Hz, 1 H), 7.08 (d,  $J$  = 9.0 Hz, 2 H), 6.84 (d,  $J$  = 8.5 Hz, 2 H), 3.78 (s, 3 H), 2.67–2.64 (m, 1 H), 2.36–2.24 (m, 1H), 1.95–1.78 (m, 1 H) ppm; MS (low res) 195.1.

**10/11- $\text{OMe}$ .** A colorless oil was recovered after flash chromatography:  $^1\text{H}$  NMR (500 MHz,  $\text{CDCl}_3$ )  $\delta$  = 9.67 (t,  $J$  = 2.0 Hz, 1 H), 7.09 (d,  $J$  = 8.5 Hz, 2 H), 6.84 (d,  $J$  = 8.5 Hz, 2 H), 3.78 (s, 3 H), 3.06–3.00 (m, 1 H), 2.67 (dd,  $J$  = 2.0, 7.5 Hz, 2 H), 1.68–1.64 (m, 1H), 1.59–1.54 (m, 1 H) ppm; MS (low res) 195.1.

**12.** A colorless oil was recovered after flash chromatography: yield 54% (71 mg);  $^1\text{H}$  NMR (500 MHz,  $\text{CDCl}_3$ )  $\delta$  = 9.71 (t,  $J$  = 1.5 Hz, 1 H), 7.96 (d,  $J$  = 8.0 Hz, 2 H), 7.19 (d,  $J$  = 8.0 Hz, 2 H), 3.90 (s, 3 H), 2.50–2.44 (m, 1 H), 2.34 (d,  $J$  = 7.5 Hz, 2 H), 1.73–1.65 (m, 2 H), 1.61–1.49 (m, 3 H), 1.23–1.06 (m, 2 H), 0.75 (t,  $J$  = 7.5 Hz, 3 H) ppm; MS (low res) 263.1.

**13.** A colorless oil was recovered after flash chromatography: yield 31% (32 mg);  $^1\text{H}$  NMR (500 MHz,  $\text{CDCl}_3$ )  $\delta$  = 7.95 (d,  $J$  = 8.0 Hz, 2H), 7.18 (d,  $J$  = 8.0 Hz, 2 H), 3.88 (s, 3 H), 2.52–2.46 (m, 1H), 2.30–2.18 (m, 1 H), 2.07–2.00 (m, 1 H), 1.85–1.77 (m, 1 H), 1.75–1.66 (m, 1 H), 1.63–1.54 (m, 1 H), 0.75 (t,  $J$  = 7.5 Hz, 3 H) ppm; MS (low res) 236.2.

**13- $\text{OH}$ .** A colorless oil was recovered after flash chromatography: yield 86% (28 mg);  $^1\text{H}$  NMR (500 MHz,  $\text{CDCl}_3$ )  $\delta$  = 7.94 (d,  $J$  = 8.0 Hz, 2H), 7.20 (d,  $J$  = 8.0 Hz, 2 H), 3.88 (s, 3 H), 3.52 (d,  $J$  = 6.5 Hz, 1 H), 2.51–2.45 (m, 1H), 1.77–1.66 (m, 2 H), 1.62–1.53 (m, 2 H), 1.42–1.37 (m, 1 H), 0.74 (t,  $J$  = 7.5 Hz, 3 H) ppm.

**14.** A colorless oil was recovered after flash chromatography: yield 26% (34 mg);  $^1\text{H}$  NMR (500 MHz,  $\text{CDCl}_3$ )  $\delta$  = 9.67 (t,  $J$  = 1.5 Hz, 1 H), 7.95 (d,  $J$  = 8.5 Hz, 2H), 7.19 (d,  $J$  = 8.0 Hz, 2 H), 3.90 (s, 3 H), 3.55 (d,  $J$  = 6.0 Hz, 1H), 2.50–2.44 (m, 1 H), 1.73–1.63 (m, 2H), 1.61–1.50 (m, 2H), 1.47–1.43 (m, 1H), 1.36–1.05 (m, 4H), 0.75 (t,  $J$  = 7.5 Hz, 3 H) ppm. MS (low res): 263.1.

**14- $\text{OH}$ .** A colorless oil was recovered after flash chromatography: yield 82% (28 mg);  $^1\text{H}$  NMR (500 MHz,  $\text{CDCl}_3$ )  $\delta$  = 7.96 (d,  $J$  = 8.5 Hz, 2H), 7.20 (d,  $J$  = 8.0 Hz, 2 H), 3.90 (s, 3 H), 3.55 (d,  $J$  = 6.0 Hz, 1H), 2.50–2.44 (m, 1 H), 1.73–1.63 (m, 2H), 1.61–1.50 (m, 2H), 1.47–1.43 (m, 1H), 1.36–1.05 (m, 4H), 0.75 (t,  $J$  = 7.5 Hz, 3 H) ppm.

**18/19.** A colorless oil was recovered after flash chromatography: yield 42% (26 mg);  $^1\text{H}$  NMR (300 MHz,  $\text{CDCl}_3$ )  $\delta$  = 9.64 (t,  $J$  = 2.0 Hz, 1 H), 7.95 (d,  $J$  = 8.0 Hz, 2 H), 7.18 (d,  $J$  = 8.0 Hz, 2 H), 3.88 (s, 3 H), 2.63–2.54 (m, 1 H), 2.26–2.18 (m, 1 H), 1.81–1.76 (m, 1 H), 1.67–1.50 (m, 2 H), 1.21–1.03 (m, 2 H), 0.82 (t,  $J$  = 7.2 Hz, 3 H) ppm; MS (low res) 250.2.



(18/19-OH). A colorless oil was recovered after flash chromatography: yield 30% (3.6 mg);  $^1\text{H}$  NMR (300 MHz,  $\text{CDCl}_3$ )  $\delta$  = 7.96 (d,  $J$  = 8.0 Hz, 2 H), 7.21 (d,  $J$  = 8.0 Hz, 2 H), 3.90 (s, 3 H), 3.56 (d,  $J$  = 6.5 Hz, 2 H), 2.62–2.56 (m, 1 H), 1.67–1.48 (m, 2 H), 1.46–1.38 (m, 1 H), 1.35–1.28 (m, 1 H), 1.22–1.08 (m, 2 H), 0.84 (t,  $J$  = 7.2 Hz, 3 H) ppm.  $^{13}\text{C}\{^1\text{H}\}$  NMR (500 MHz,  $\text{CDCl}_3$ )  $\delta$  = 167.4, 151.7, 129.9, 127.9, 126.0, 63.1, 52.2, 45.9, 39.2, 32.5 (t,  $J$  = 76.5 Hz), 30.5 (t,  $J$  = 76.0 Hz), 29.9, 20.8, 14.3 ppm; IR (neat) 3421, 2955, 2925, 2872, 1721, 1653, 1610, 1559, 1507, 1457, 1436, 1418, 1378, 1180, 1112, 1049, 967, 857, 774, 709, 668  $\text{cm}^{-1}$ ; HRMS (ESI-TOF)  $m/z$  [ $\text{M} + \text{Na}$ ] $^+$  calcd for  $\text{C}_{13}\text{H}_{16}\text{D}_2\text{O}_3\text{Na}$  275.1592, found 275.1598.

**General Procedure for Cyclization of Isolated Heck Products.** Aldehyde product was oxidized to the corresponding carboxylic acid by stirring with oxone (2 equiv) in DMF (3 mL) for 18 h. The reaction mixture was quenched with 1 M HCl (10 mL) and ether (10 mL). The layers were separated, and the aqueous layer was extracted with ether (3  $\times$  10 mL). The combined organic layers were washed with 1 M HCl (1  $\times$  10 mL) and brine (2  $\times$  10 mL), dried over magnesium sulfate, and concentrated under reduced pressure. The isolated acid was dissolved in dichloromethane (10 mL) and cooled in an ice bath. Oxalyl chloride (2 equiv) was added, and the reaction was stirred at 0  $^\circ\text{C}$  for 3 h. The reaction was diluted with dichloromethane (40 mL), and aluminum chloride (2 equiv) was added. The reaction mixture stirred overnight and was quenched with water (20 mL). The layers were separated, and the aqueous layer was extracted with dichloromethane (3  $\times$  10 mL). The combined organic layers were washed with brine (3  $\times$  10 mL), dried over magnesium sulfate, and concentrated under reduced pressure. The crude mixture was purified using flash chromatography.

**15.** A colorless oil was recovered after flash chromatography: yield over two steps 46% (0.27 g);  $R_f$  (80:20 EtOAc/hexanes) = 0.53;  $^1\text{H}$  NMR (500 MHz,  $\text{CDCl}_3$ )  $\delta$  = 8.65 (d,  $J$  = 2.0 Hz, 1 H), 8.14 (dd,  $J$  = 8.2, 2.0 Hz, 1 H), 7.37 (d,  $J$  = 8.0 Hz, 1 H), 3.91 (s, 3 H), 2.90–2.87 (m, 1 H), 2.79–2.75 (m, 1 H), 2.60 (dt,  $J$  = 17.5, 5.0 Hz, 1 H), 2.26–2.22 (m, 1 H), 2.09 (dq,  $J$  = 13.8, 5.0 Hz, 1 H), 1.80–1.70 (m, 2 H), 1.02 (t,  $J$  = 7.5 Hz, 3 H) ppm;  $^{13}\text{C}\{^1\text{H}\}$  NMR (125 MHz,  $\text{CDCl}_3$ )  $\delta$  = 197.7, 166.6, 153.1, 134.0, 132.2, 129.1, 128.9, 52.4, 40.0, 35.0, 27.5, 26.2, 12.3 ppm; IR (neat) 3853, 3838, 3744, 3735, 3711, 3689, 3676, 3649, 3629, 2955, 2875, 1720, 1687, 1653, 1636, 1609, 1559, 1540, 1521, 1489, 1457, 1436, 1418, 1303, 1243, 1190, 1111, 975, 918, 859, 763, 668, 651  $\text{cm}^{-1}$ ; HRMS (ESI-TOF)  $m/z$  [ $\text{M} + \text{Na}$ ] $^+$  calcd for  $\text{C}_{14}\text{H}_{16}\text{O}_3\text{Na}$  255.0997, found 255.1003.

**16.** A colorless oil was recovered after flash chromatography: yield over two steps 49% (0.11 g);  $^1\text{H}$  NMR (500 MHz,  $\text{CDCl}_3$ )  $\delta$  = 8.67 (d,  $J$  = 2.0 Hz, 1 H), 8.15 (dd,  $J$  = 8.0, 2.0 Hz, 1 H), 7.38 (d,  $J$  = 8.0 Hz, 1 H), 3.92 (s, 3 H), 2.77 (dd,  $J$  = 5.0, 17.8 Hz, 1 H), 2.62 (dd,  $J$  = 5.5, 17.5 Hz, 1 H), 2.22 (dd,  $J$  = 4.0, 11.5 Hz, 1 H), 1.80–1.68 (m, 2 H), 1.03 (t,  $J$  = 7.5 Hz, 3 H) ppm.

**17.** A colorless oil was recovered after flash chromatography: yield over two steps 32% (0.10 g);  $^1\text{H}$  NMR (500 MHz,  $\text{CDCl}_3$ )  $\delta$  = 8.65 (d,  $J$  = 3.0 Hz, 1 H), 8.13 (dd,  $J$  = 8.0, 3.0 Hz, 1 H), 7.37 (d,  $J$  = 8.0 Hz, 1 H), 3.91 (s, 3 H), 2.76 (dd,  $J$  = 12.0, 18.0 Hz, 1 H), 2.60 (dd,  $J$  = 5.0, 18.0 Hz, 1 H), 2.07 (t,  $J$  = 5.0 Hz, 1H), 1.80–1.68 (m, 2 H), 1.02 (t,  $J$  = 7.5 Hz, 3 H) ppm.

**20/21.** A colorless oil was recovered after flash chromatography: yield over two steps 67% (0.14 g);  $R_f$  (80:20 hexanes/ethyl acetate) = 0.39;  $^1\text{H}$  NMR (500 MHz,  $\text{CDCl}_3$ )  $\delta$  = 8.67 (s, 1 H), 8.14 (d,  $J$  = 8.0, 1 H), 7.36 (d,  $J$  = 8.0 Hz, 1 H), 3.92 (s, 3 H), 3.00–2.96 (m, 1 H), 2.78 (dd,  $J$  = 4.5, 18 Hz, 0.55 H), 2.60 (dd,  $J$  = 5.5, 18 Hz, 0.72 H), 2.07–2.02 (m, 1H), 1.68 (q,  $J$  = 8.0 Hz, 2 H), 1.53–1.33 (m, 2 H), 0.97 (t,  $J$  = 7. Hz, 3 H) ppm;  $^{13}\text{C}\{^1\text{H}\}$  NMR (125 MHz,  $\text{CDCl}_3$ )  $\delta$  = 197.8, 166.6, 153.5, 134.0, 132.1, 130.4, 129.1, 127.5, 52.5, 38.1, 36.9, 34.5 (q,  $J$  = 78.5 Hz), 26.1 (m), 20.9, 14.3 ppm; IR (neat) 2955, 2931, 2872, 1720, 1686, 1608, 1457, 1435, 1415, 1300, 1228, 1104, 962, 930, 852, 767, 668, 540  $\text{cm}^{-1}$ ; HRMS (ESI-TOF)  $m/z$  [ $\text{M} + \text{Na}$ ] $^+$  calcd for  $\text{C}_{15}\text{H}_{16}\text{D}_2\text{O}_3\text{Na}$  271.1279, found 271.1281.

**Computational Details.** The M06 functional<sup>19</sup> implemented in Gaussian09.C01<sup>20</sup> is used in unconstrained geometry optimization and frequency calculation. The LANL2DZ+ $f^{21}$  and 6-31+G(d) basis sets were used for Pd and all other atoms, respectively. Single-point

calculations using the SDD basis set for Pd and the 6-311++G(d, p) basis set for all other atoms and the SMD solvent model with the parameters for DMF were used to account for solvent effects. The final free energies from the single-point calculations with solvent and thermal corrections are reported in kcal/mol at standard conditions. Kinetic isotope effects were estimated from the M06/LAN2DZ/6-31+G(d) free energies and corrected for hydrogen tunneling using the one-dimensional approximation proposed by Bell.<sup>22</sup> Figures of the key transition structures were prepared using CYLView.<sup>23</sup>

## ■ ASSOCIATED CONTENT

### 📄 Supporting Information

Supplementary figures, determination of relative stereochemistry, NMR spectra, and optimized Cartesian coordinates and energies. This material is available free of charge via the Internet at <http://pubs.acs.org>.

## ■ AUTHOR INFORMATION

### ✉ Corresponding Author

\*E-mail: [sigman@chem.utah.edu](mailto:sigman@chem.utah.edu).

### 📄 Notes

The authors declare no competing financial interest.

## ■ ACKNOWLEDGMENTS

This work was supported by the National Institutes of Health (NIGMS RO1 GM063540), the National Science Foundation of China (21133002, 21232001), the MOST of China (2013CB911501), the Shenzhen Peacock Program (KQTD201103), and NSF CHE 1058075. L.-P.X. acknowledges support from the Graduate School of Peking University for international exchange.

## ■ REFERENCES

- (1) Werner, E. W.; Mei, T.-S.; Burckle, A. J.; Sigman, M. S. *Science* **2012**, *338*, 1455.
- (2) Mei, T.-S.; Werner, E. W.; Burckle, A. J.; Sigman, M. S. *J. Am. Chem. Soc.* **2013**, *135*, 6830.
- (3) For selected examples using a redox-relay strategy, see: (a) Renata, H.; Zhou, Q.; Baran, P. S. *Science* **2013**, *339*, 59. (b) Burns, N. Z.; Baran, P. S.; Hoffmann, R. W. *Angew. Chem., Int. Ed.* **2009**, *48*, 2854.
- (4) Milo, A.; Bess, E. N.; Sigman, M. S. *Nature* **2014**, *507*, 210.
- (5) Mei, T.-S.; Patel, H. H.; Sigman, M. S. *Nature* **2014**, *508*, 340.
- (6) Dang, Y.; Qu, S.; Wang, Z.-X.; Wang, X. *J. Am. Chem. Soc.* **2013**, *136*, 986.
- (7) Xu, L.; Hilton, M. J.; Zhang, X.; Norrby, P.-O.; Wu, Y.-D.; Sigman, M. S.; Wiest, O. *J. Am. Chem. Soc.* **2014**, *136*, 1960.
- (8) Tempel, D. J.; Johnson, L. K.; Huff, R. L.; White, P. S.; Brookhart, M. *J. Am. Chem. Soc.* **2000**, *122*, 6686.
- (9) Shultz, L. H.; Brookhart, M. *Organometallics* **2001**, *20*, 3975.
- (10) Shultz, L. H.; Tempel, D. J.; Brookhart, M. *J. Am. Chem. Soc.* **2001**, *123*, 11539.
- (11) Arnett, E. M. *Prog. Phys. Org. Chem.* **1963**, *1*, 223.
- (12) McMullin, C. L.; Jover, J.; Harvey, J. N.; Fey, N. *Dalton Trans.* **2010**, *39*, 10833–10836.
- (13) Willoughby, P. H.; Jansma, M. J.; Hoye, T. R. *Nat. Protoc.* **2014**, *9*, 643.
- (14) Drent, E.; van Broekhoven, J. A. M.; Doyle, M. J. *J. Organomet. Chem.* **1991**, *417*, 235.
- (15) Zeng, J.; Deng, G.; Li, D. *Biochim. Biophys. Acta, Gen. Subj.* **2006**, *1760*, 78.
- (16) Hudrlik, P. F.; Hudrlik, A. M.; Yimenu, T.; Waugh, M. A.; Nagendrappa, G. *Tetrahedron* **1988**, *44*, 3791.
- (17) Luehr, G. W.; Arathi, S.; Jaishankar, P.; Bhakta, C.; Druzgala, P. *PTC Int. Appl.*, 2010071813, Ed. 2010.

- (18) Kim, A. I.; Rychnovsky, S. D. *Angew. Chem., Int. Ed.* **2003**, *42*, 1267.
- (19) Zhao, Y.; Truhlar, D. G. *Theor. Chem. Acc.* **2008**, *120*, 215.
- (20) Frisch, M. J., et al. Gaussian Inc.: Wallingford, CT, 2009.
- (21) Ehlers, A. W.; Böhme, M.; Dapprich, S.; Gobbi, A.; Höllwarth, A.; Jonas, V.; Köhler, K. F.; Stegmann, R.; Veldkamp, A.; Frenking, G. *Chem. Phys. Lett.* **1993**, *208*, 111.
- (22) Bell, R. P. *The Tunnel Effect in Chemistry*; Chapman and Hall: New York, 1980.
- (23) Legault, C. Y. <http://www.cylvview.org>, Université de Sherbrooke, 2009.